

Supplementary information

Novel Hierarchical Porous Carbon Prepared By One-step Template Routing for Electric Double Layer Capacitors and Li-Se Battery Devices

Youyi Lei,^{a, b} Xinmiao Liang*,^a Li Yang,^{a, b} Ping Jiang,^{a, b} Zhenyu Lei,^{a, b} Shuaishuai Wu,^{a, b} and
Jiwen Feng *^a

^aState Key Laboratory of Magnetic Resonance and Atomic Molecular Physics, National Center for
Magnetic Resonance in Wuhan, Key Laboratory of Magnetic Resonance in Biological Systems, Wuhan
Institute of Physics and Mathematics, Chinese Academy of Sciences, Wuhan 430071; P. R. China

^bUniversity of Chinese Academy of Sciences, Beijing 100000, P.R. China

* Corresponding author. E-mail: xmliang@wipm.ac.cn.

* Corresponding author. E-mail: jwfeng@wipm.ac.cn.

We can make a simple metaphor of energy density and power density. Energy density is like a reservoir and the power density is like a valve. In the microporous carbon electrode, the larger the valve is opened, the water storage amount will be significantly reduced; in the mesoporous carbon, although the size of the valve does not affect the water reserve, the inherent reserve of water is low. The hierarchical porous carbon solves the contradiction between the reserve and the valve, so that the water reserve of the activated carbon electrode is increased, and only slightly fluctuates with the change of the valve size.

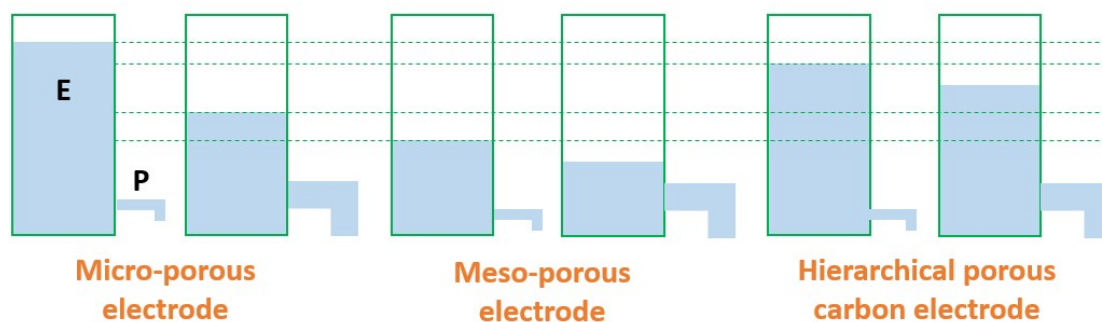


Figure S1. Schematic of energy density and power density of different types of porous carbon in EDLC model.

In the three-electrode system, foamed nickel was used as the current collector, the Hg-HgO electrode and the platinum column are used as the reference electrode and the auxiliary electrode, respectively, and 6M KOH was the electrolyte. The specific capacitance was calculated as:

$$C_s = \frac{I \times \Delta t}{m \times \Delta V} \quad (1)$$

where I is the current (A), Δt is the discharge time (s), m is the active carbon mass of single electrodes (g) and ΔV represents the potential window.

In a two-electrode system, a foamed nickel current collector coated with activated carbon and a glass fiber membrane were assembled into a CR2032 button cell. The cell capacitance under this system was based on the following calculation method:

$$C_{cell} = \frac{I \times \Delta t}{m \times \Delta V} \quad (2)$$

where I is the current (A), Δt is the discharge time (s), m is the total mass of both carbon electrodes (g) and ΔV represents the cell voltage.

In addition, the power density (P) and energy density (E) are calculated as follows:

$$E = \frac{1}{2} C_{cell} V^2 \quad (3)$$

$$P = \frac{E}{\Delta t} \quad (4)$$

where C is the cell capacitance of the device, V is the operating voltage and Δt is the discharge time (s).

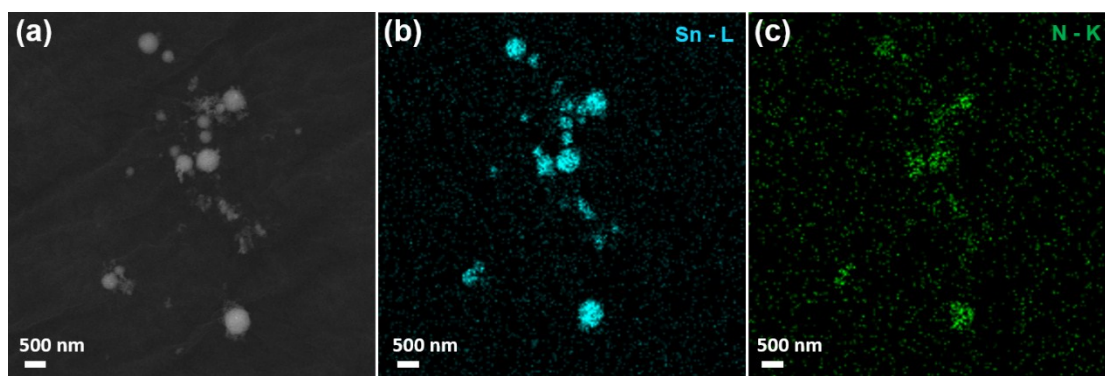


Figure S2. (a) SEM image of mapping area of $\text{SnO}_2@\text{CIS-29}$. (b, c) EDS image of Sn and N elements distribution.

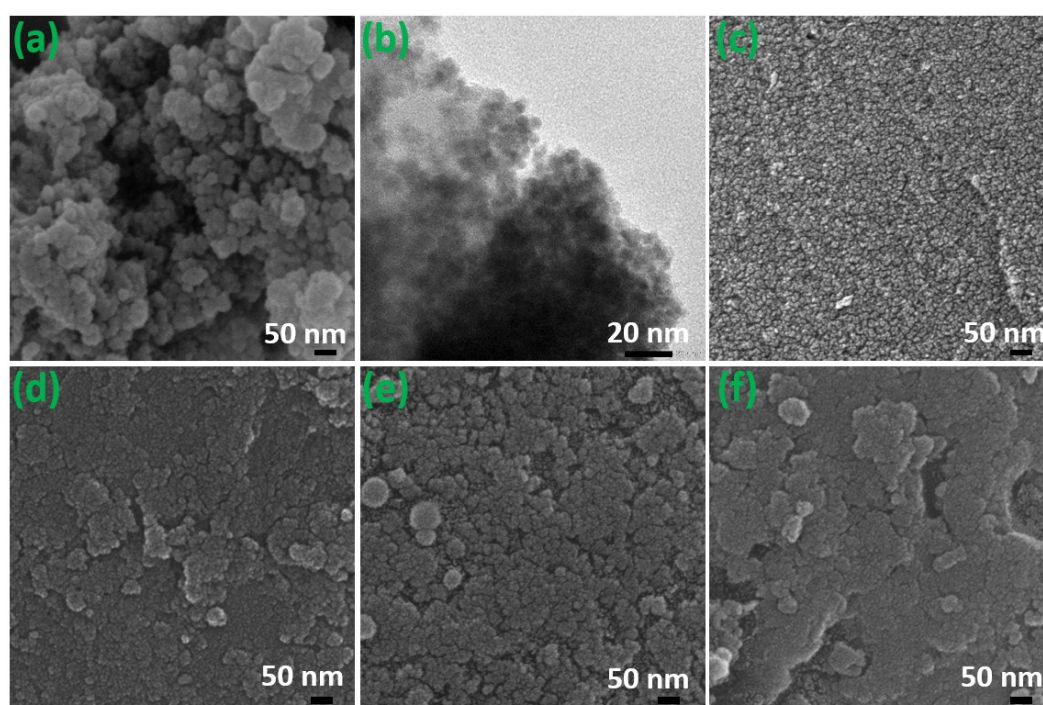


Figure S3. Electronic imaging of composite and hierarchical porous carbon. (a) SEM images of $\text{CIS-29}@\text{SnO}_2$. (b) TEM images of $\text{CIS-29}@\text{SnO}_2$. (c, e, f and g) SEM images of CISC-00, CISC-29, CISC-58 and CISC-87.

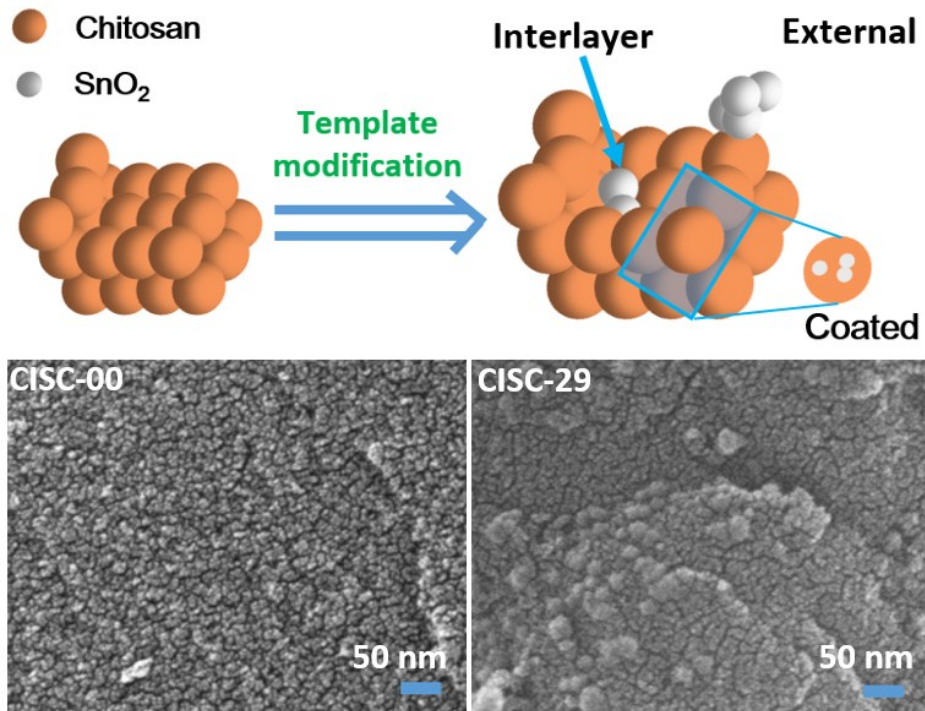


Figure S4. The nucleation between the layers of tin dioxide causes a large number of cracks on the surface of the hierarchical porous carbon.

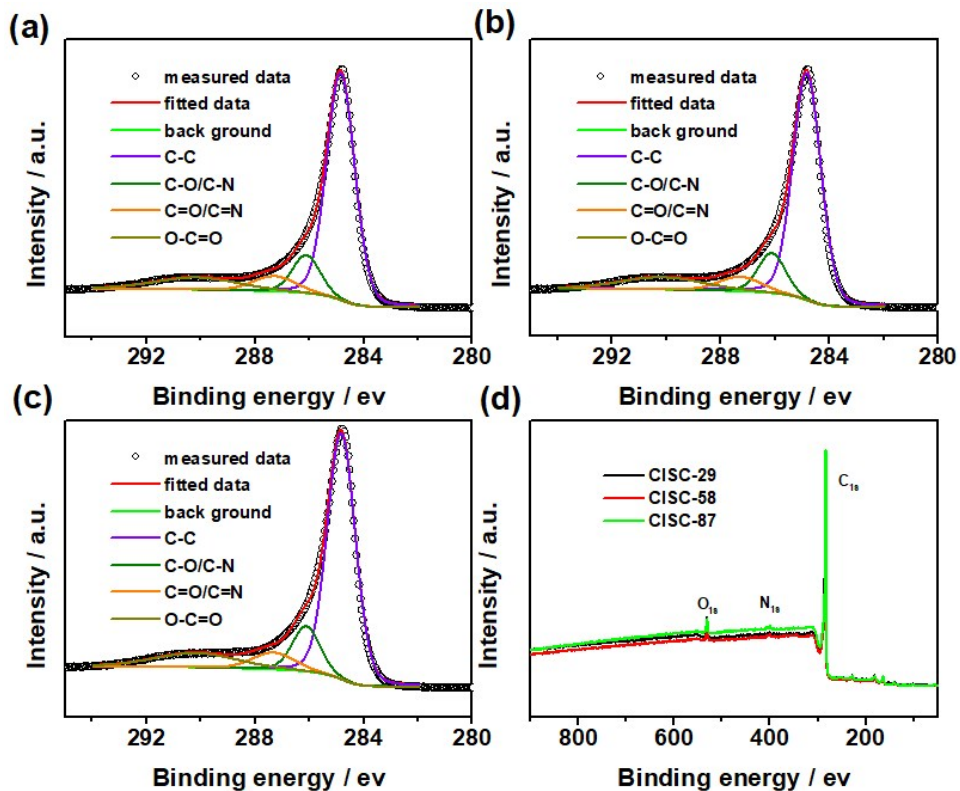


Figure S5 (a,b and c) Peak fitting of C1s in CISC-29, CISC-58 and CISC-87, respectively. (d) XPS spectroscopy of CISC-29, CISC-58 and CISC-87.

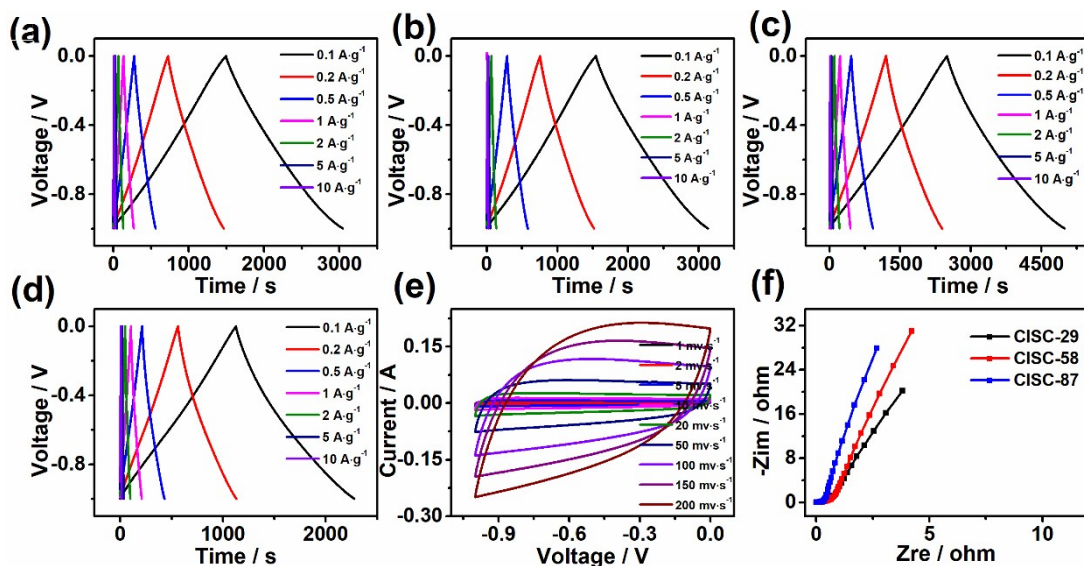


Figure S6. (a, b, c and d) Galvanostatic charge and discharge profiles of CISC-87, CISC-58, CISC-29 and CISC-00 under three-electrode system. (e) CV curve of CISC-29 under three-electrode system. (f) EIS spectrum of CISC-29, CISC-58 and CISC-87 electrode.

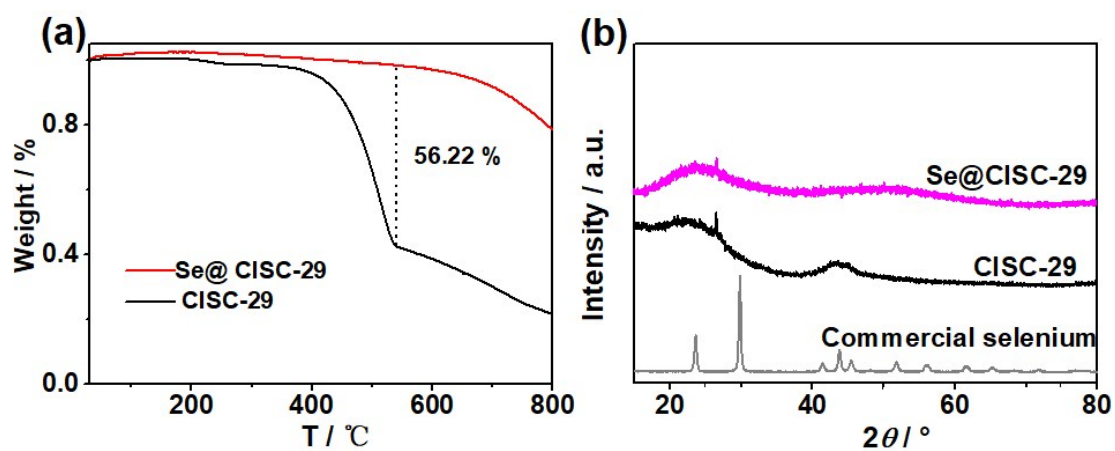


Figure S7. (a) TG of Se@CISC-29 and CISC-29 (b) XRD pattern of commercial selenium, CISC-29 and Se@CISC-29.

Table S1. Elemental content of CISC-29, CISC-58 and CISC-87.

	C(%)	O(%)	N(%)
CISC-29	94.5	4.6	0.9
CISC-58	96.3	2.5	1.2
CISC-87	96.4	2.8	0.8

Table S2. Specific surface area and pore volume information (calculated by NLDFT) of CISC-00, CISC-29, CISC-58 and CISC-87.

	CISC-00	CISC-29	CISC-58	CISC-87
$S_{\text{BET}} / \text{m}^2 \cdot \text{g}^{-1}$	747.66	1391.02	1548.92	1570.95
$V_{\text{pore}} / \text{cm}^3 \cdot \text{g}^{-1}$	0.40	0.88	1.01	1.04
$V_{\text{micro-pore}} / \text{cm}^3 \cdot \text{g}^{-1}$	0.40	0.64	0.70	0.69
$V_{\text{meso-pore}} / \text{cm}^3 \cdot \text{g}^{-1}$	0	0.1	0.15	0.2